

Article

Fault Current Limiting Characteristics of a Small-Scale Bridge Type SFCL with Single HTSC Element Using Flux-Coupling

Tae-Hee Han ¹, Seok-Cheol Ko ² and Sung-Hun Lim ^{3,*}

¹ Department of Aero Materials Engineering, Jungwon University, Chungbuk 28024, Korea; hantaehee@jwu.ac.kr

² Industry-University Cooperation Foundation, Kongju National University, Chungnam 32586, Korea; suntrac@kongju.ac.kr

³ Department of Electrical Engineering, Soongsil University, 369, Sangdo-ro, Dongjak-gu, Seoul 06978, Korea

* Correspondence: superlsh73@ssu.ac.kr; Tel.: +82-2-828-7268

Received: 22 February 2020; Accepted: 24 March 2020; Published: 28 March 2020



Abstract: In this paper, a bridge type superconducting fault current limiter (SFCL) with a single high-temperature superconducting (HTSC) element is proposed to allow fault current limiting operation in direct current (DC) conditions. First, the principle of operation of the bridge type SFCL with a single HTSC element using flux-coupling was presented. After the fault occurrence, the fault current limiting operation and voltage characteristics, the power load characteristics of each device, and the energy consumption of the two coils and the HTSC element were analyzed in the proposed SFCL. As a result, it is confirmed that in the case of the additive polarity winding, the power consumption and the energy consumption of the HTSC element were lower than those in the subtractive polarity winding, and the fault current limiting characteristics were excellent.

Keywords: bridge type; HTSC element; flux-coupling; fault current limiting operation; Superconducting fault current limiter (SFCL)

1. Introduction

Today, power distribution facilities in low-voltage systems utilize a switching arc function to control fault current. Power utilities in high voltage systems typically operate with special switchgear, and their components are designed to withstand fault currents before the circuit opens. Power distribution facilities should be equipped with a protection system in case of a short circuit in the grid voltage. The protection system has a small internal resistance during normal operation, but in the event of an accident, it must generate a high impedance within a very short time to limit the short-circuit current and return to normal operation mode immediately after the fault is resolved. A device that can have this function is a superconducting fault current limiter (SFCL) [1,2]. This is because such a function can be provided by changing from a zero resistance to a high normal resistance when the critical current, critical temperature, and critical magnetic field are exceeded. For this reason, numerous SFCLs have been proposed in the past few years [3–6]. SFCL technology with high-efficiency and high-compression design was introduced almost 50 years ago [7].

SFCLs can be classified into resistance type, bridge type, self-shielding type, and saturated core type according to the structure and operating principle [8–11]. Among them, the bridge type SFCL uses a diode or thyristor as a Graetz bridge connected to a superconducting coil [12,13]. When normal power is applied to the power system, the voltage across the diode is determined by the diode's internal resistance, and its value is very small. For this reason, the polarity does not change as determined by

the direct current (DC) power supply. Since the four diodes are forward biased, each circuit operates independently of each other.

When a short circuit accident occurs in the power system, the voltage across each diode is increased tens of times compared to the normal state. Therefore, in the normal state, two of the forward biases applied to the diode are subjected to the reverse bias, whereby the two circuits that were previously independent affect each other. The alternating current (AC) affects the DC power supply and a fault current flows through the coil. Here, the fault current does not increase rapidly due to the inductance of the coil, but gradually increases, so that even if a short circuit accident occurs, it does not significantly affect the system at the beginning. In this way, the system can be protected when the circuit break (CB) is operated in a situation where the current is not increased to disconnect the circuit from the power supply.

When limiting the fault current, the inductor may be normal, but there is always some current flowing and significant continuous loss. This can be avoided by using a superconducting coil. Fault current can be limited by using an iron core inductor, but a large amount of iron is required to prevent saturation. The Graetz bridge must have a power capacity to accommodate the losses, so the losses are much less when using superconducting inductors. Recently, a bridge type SFCL applied with a thyristor or an insulated gate bipolar transistor (IGBT) switch instead of a diode, and a DC resistance type in which a superconducting coil capable of being quenched is added to the diode bridge has been proposed [14–25]. However, this type of SFCL has the disadvantage of being larger than other types of SFCL due to the superconducting coil. The SFCL also requires an additional controller and CB to protect the superconducting coil from accidents.

In order to overcome these drawbacks, we would like to propose a bridge type SFCL with a single high-temperature superconducting (HTSC) element using flux-coupling that can utilize an AC or DC system. The fault current limiting operation characteristics of the bridge type SFCL were analyzed. When the connection direction between the two coils was different during the fault cycle, the fault current limiting operation due to the quench of a single HTSC element, the voltage characteristics of each element, the magnetic flux and instantaneous power of two windings, and the energy consumption were compared with each other.

2. Structure and Operating Principle

2.1. Structure and Principle

Figure 1 shows the structure of a bridge type SFCL with a single HTSC element using flux-coupling between two windings. The SFCL consists of four diodes connected in the form of full-wave bridges for operation at DC, two coils wound around one iron core, and a HTSC element connected to only one coil in series. The winding direction between the primary and secondary windings (N_1 , N_2) can be changed to either subtractive polarity winding or additive polarity winding. The HTSC element was $Y_1Ba_2Cu_3O_{7-x}$ (YBCO) thin films deposited with a 200 nm thick layer of platinum and was a product of Theva, Germany.

The basic operation principle is that the resistance of the HTSC element becomes zero because no quenching occurs under conditions prior to the failure. In addition, since the current flowing through the N_1 and N_2 windings is DC, these two coils are bypassed so that no magnetic flux occurs. Of course, even if AC ripple occurs due to the loss of the diode, the magnetic fluxes cancel each other out and become zero.

However, after a fault has occurred, the transient fault current exceeds the critical current of the HTSC element in series with the N_2 winding, and the HTSC element has a resistance that causes a quench. The DC current flowing through the N_1 and N_2 windings causes a mixture of AC ripple components to generate magnetic flux. As a result, non-inductive coupling breaks and limits the fault current.

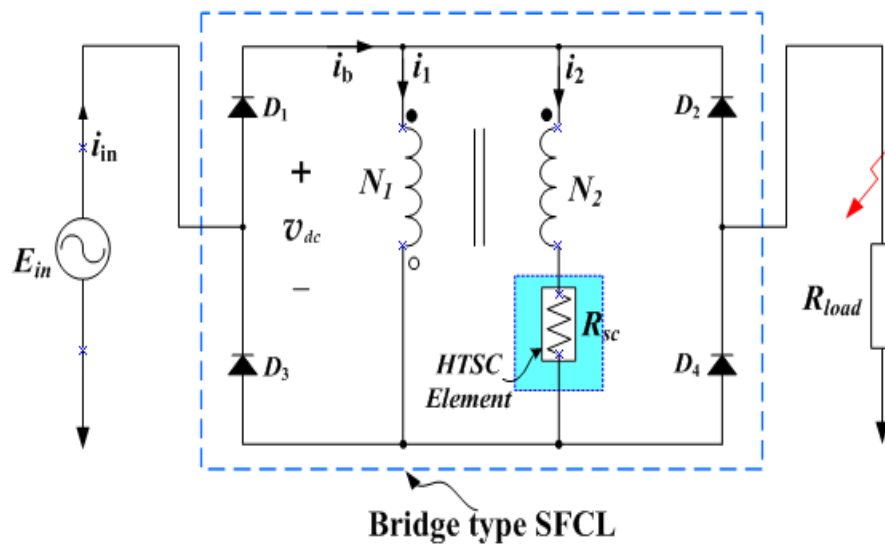


Figure 1. Schematic configuration of bridge type superconducting fault current limiter (SFCL) with a single high-temperature superconducting (HTSC) element using flux-coupling.

2.2. Equivalent Circuit

Figure 2 shows the electrical equivalent circuit of a bridge type SFCL with a single HTSC element using flux-coupling. The resistance and leakage inductance of each winding are omitted for simplicity. The inductance of the two windings is shown as L_1 and L_2 , and the resistance of the HTSC element is represented as R_{sc} when the HTSC element is quenched and resistance occurs. Depending on the wiring direction between N_1 and N_2 windings, it is divided into a subtractive polarity winding and an additive polarity winding, indicated by \bullet and \circ , respectively. In the case of a subtractive polarity winding and an additive polarity winding from the equivalent circuit of Figure 2, the fault current limiting operating current (I_{op}) can be represented by Equations (1) and (2), respectively.

$$I_{op-sub} = \frac{L_2 + \sqrt{L_1 L_2}}{L_1 + \sqrt{L_1 L_2}} \times I_c \tag{1}$$

$$I_{op-add} = \frac{L_2 - \sqrt{L_1 L_2}}{L_1 - \sqrt{L_1 L_2}} \times I_c \tag{2}$$

where I_c means the critical current.

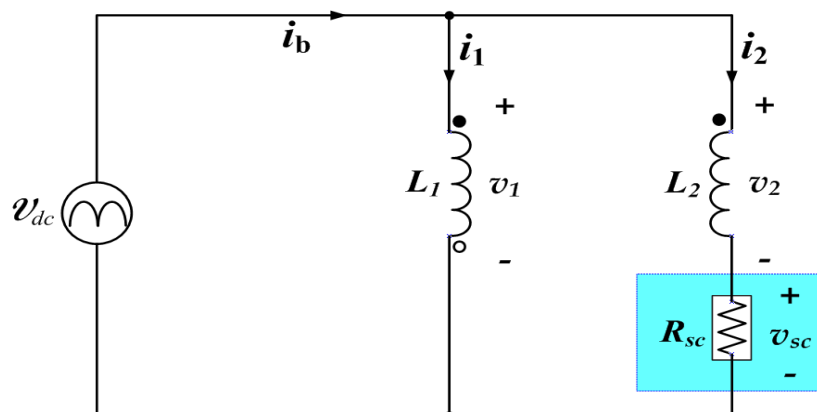


Figure 2. Equivalent circuit of bridge type SFCL with a single HTSC element using flux-coupling.

3. Experimental Results

3.1. Preparation of Experiment

The design parameters of a bridge type SFCL with a single HTSC element using flux-coupling are shown in Table 1. The HTSC element having a critical current of 18.15 A was used by patterning the YBCO thin film. The fabrication process of the HTSC element used in this experiment is reported in other previous papers [26–28].

Table 1. Specifications of bridge type SFCL with a single HTSC element using flux-coupling.

Windings (Turn Number, Self Inductance)	Value	Unit
Primary Winding (N_1, L_1)	45, 20.293	Turns, mH
Secondary Winding (N_2, L_2)	15, 1.295	Turns, mH
Iron Core (Laminated Si)	Size	Unit
Outer horizontal length	250	mm
Outer vertical length	235	mm
Inner horizontal length	155	mm
Inner vertical length	137	mm
Thickness	132	mm
HTSC Element (R_{SC})	Value	Unit
Material	YBCO	Thin Film
Critical Current (I_C)	18.15	A
Critical Temperature (T_C)	87	K
Total Meander Line Length	420	mm
Line Width	2	mm
Thin Film Thickness	0.3	μm
Gold Layer Thickness	0.2	μm

Figure 3 shows the schematic diagram of the experimental device for analyzing the fault current limiting operation characteristics, voltage waveforms, instantaneous power and magnetic flux change of a bridge type SFCL with a single HTSC element. As shown in the experimental device of Figure 3, the proposed bridge type SFCL consisted of a bridge diode, an iron core, and a superconducting element. There was no need for a controller and circuit breaker to protect against short-circuit accidents, such as the bridge type SFCL with the conventional thyristor or IGBT switch presented in the introduction. A fault short-circuit experiment was performed at 40 V_{rms} AC input voltage (E_{in}) at 60 Hz and a fault angle of 0° . The test equipment consisted of a bridge circuit to obtain full-wave rectification, a line reactance (X_{line}) of 0.6Ω , a line resistance of 1Ω (R_{line}), a load resistance of 50Ω (R_{load}), two windings on an iron core, and one HTSC element. This short-circuit tester was designed to supply AC power (E_{in}) using short-circuit SW_2 after SW_1 closed and to open the SW_1 and SW_2 after the fault cycle to cut off the power supply.

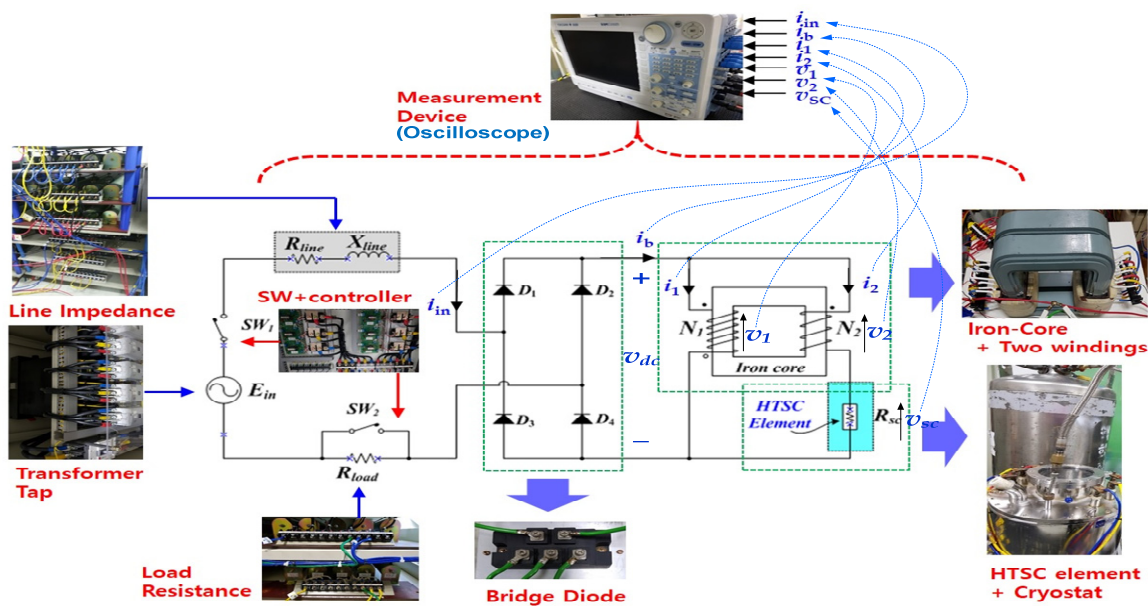


Figure 3. Short-circuit test of bridge type SFCL with a single HTSC element using flux-coupling.

3.2. Experimental Results

Figure 4 shows the fault current limiting characteristics and voltage waveforms of a bridge type SFCL with a single HTSC element using flux-coupling when the two windings are connected to the subtractive polarity winding and the additive polarity winding at the input voltage source of $40 V_{rms}$ and the fault angle of 0° . During the fault period, each fault section was subdivided into (1), (2), (3), (4), (5), and (6). The fault current (i_{in}) gradually increased immediately after the fault, but it was observed that the fault current suddenly increased before the quench occurred in the HTSC element. This phenomenon is due to the saturation of the iron core, and the fault current increases rapidly, causing quenching of the HTSC element. This proves that the fault current is limited by increasing the impedance due to the quench of the HTSC element connected in series to the secondary winding.

The experimental results were compared and analyzed according to the subtractive polarity winding and the additive polarity winding, which are the wiring directions between the primary and secondary windings. It can be seen that the voltage generated due to the quenching of the HTSC element is smaller in the case of the additive polarity winding than that of the subtractive polarity winding. In addition, it can be seen that the current (i_2) flowing through the secondary winding (N_2) is larger in the case of the additive polarity winding than that of the subtractive polarity winding from 2.5 cycles.

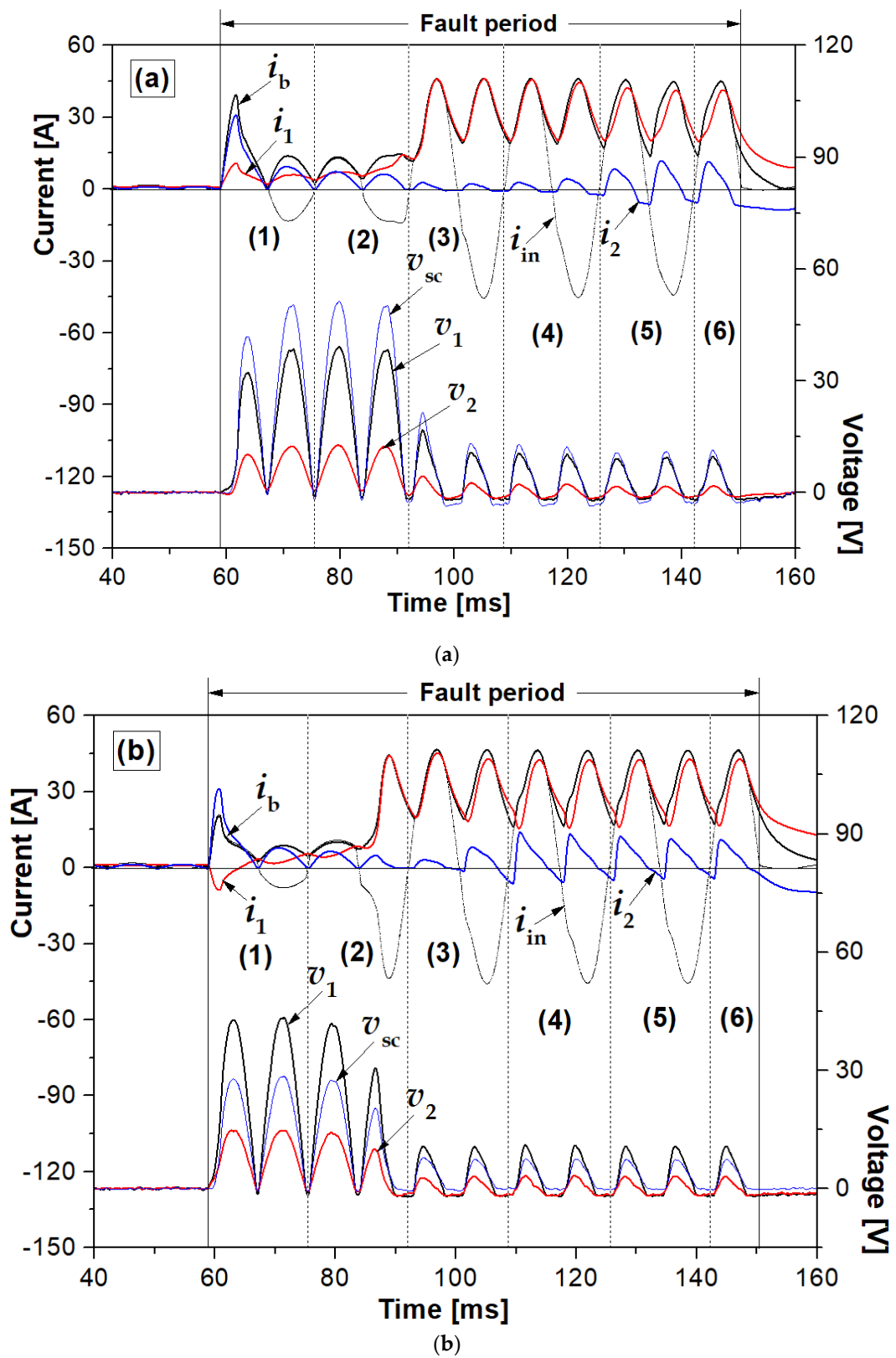


Figure 4. Fault current limiting characteristics and voltage waveforms of bridge type SFCL with a single HTSC element using flux-coupling according to the connection direction between N_1 and N_2 . (a) In the case of the subtractive polarity winding. (b) In the case of the additive polarity winding.

Figure 5 shows the instantaneous power burden characteristics of the devices and the magnetic fluxes (ϕ_1, ϕ_2) of the two windings in a bridge type SFCL with a single HTSC element using flux-coupling when the two windings are connected to the subtractive polarity winding and the additive polarity winding during the fault period. The magnetic fluxes of the primary and secondary windings were similar in magnitude, regardless of the wiring direction between the two coils. On the other hand, it can be observed that the instantaneous power consumed in the HTSC element was much larger in the case of the subtractive polarity winding than that of the additive polarity winding immediately after the failure. The reason for this is that the HTSC element connected in series to the secondary winding is quenched, and its impedance value is greater. Also, it can be seen that the instantaneous power consumed in the secondary winding is higher in the case of the additive polarity winding than that of the subtractive polarity winding immediately after the failure.

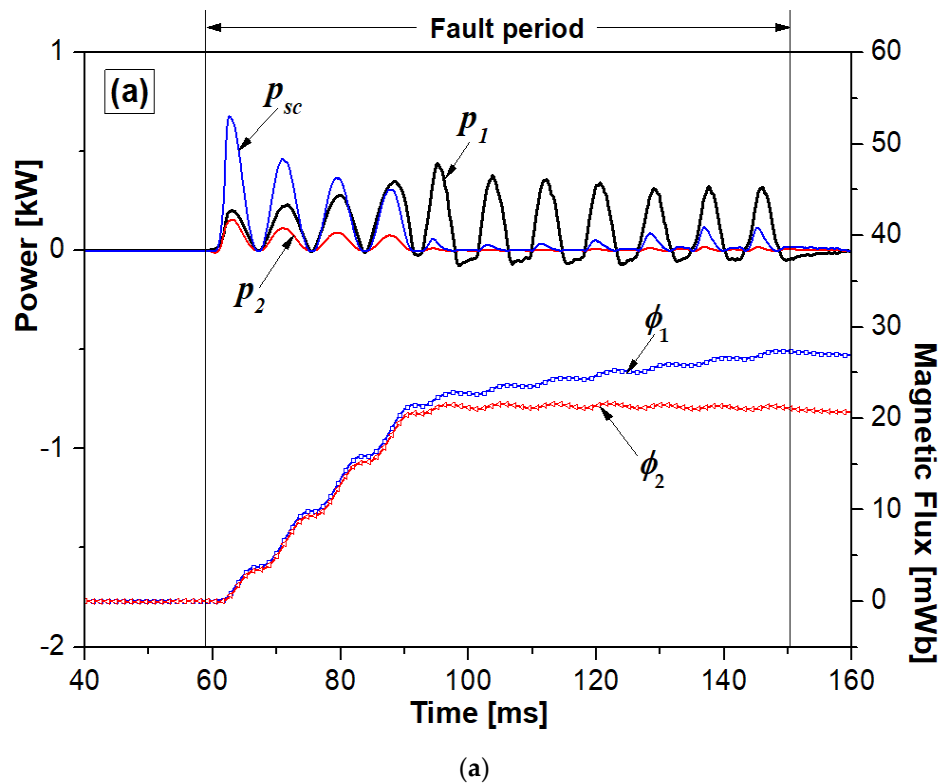


Figure 5. Cont.

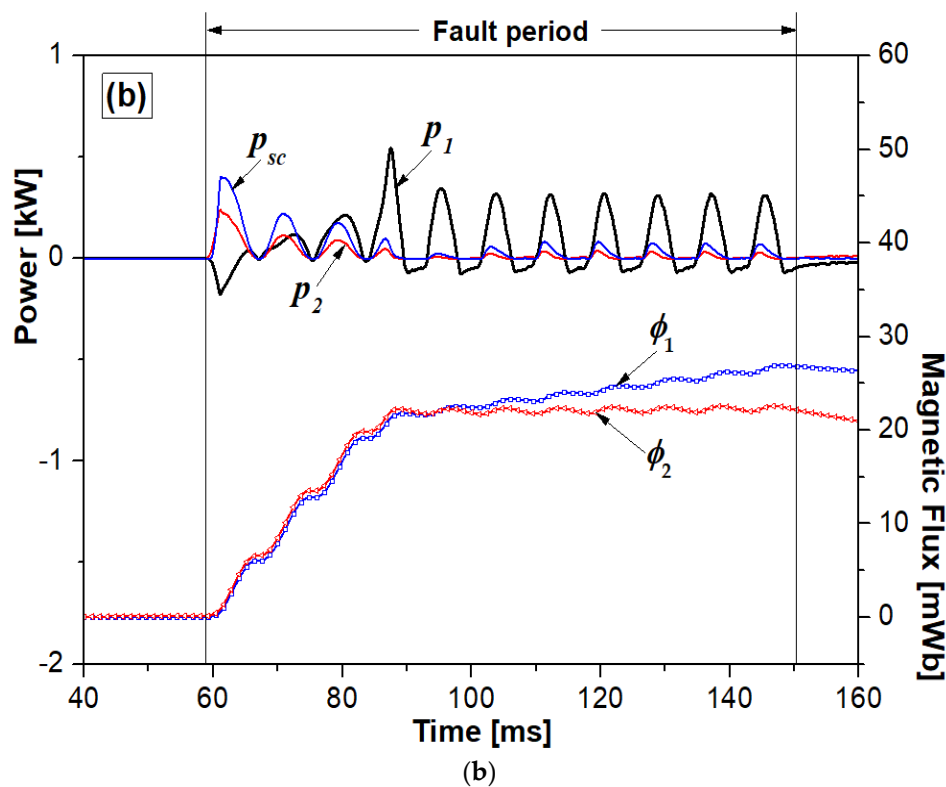
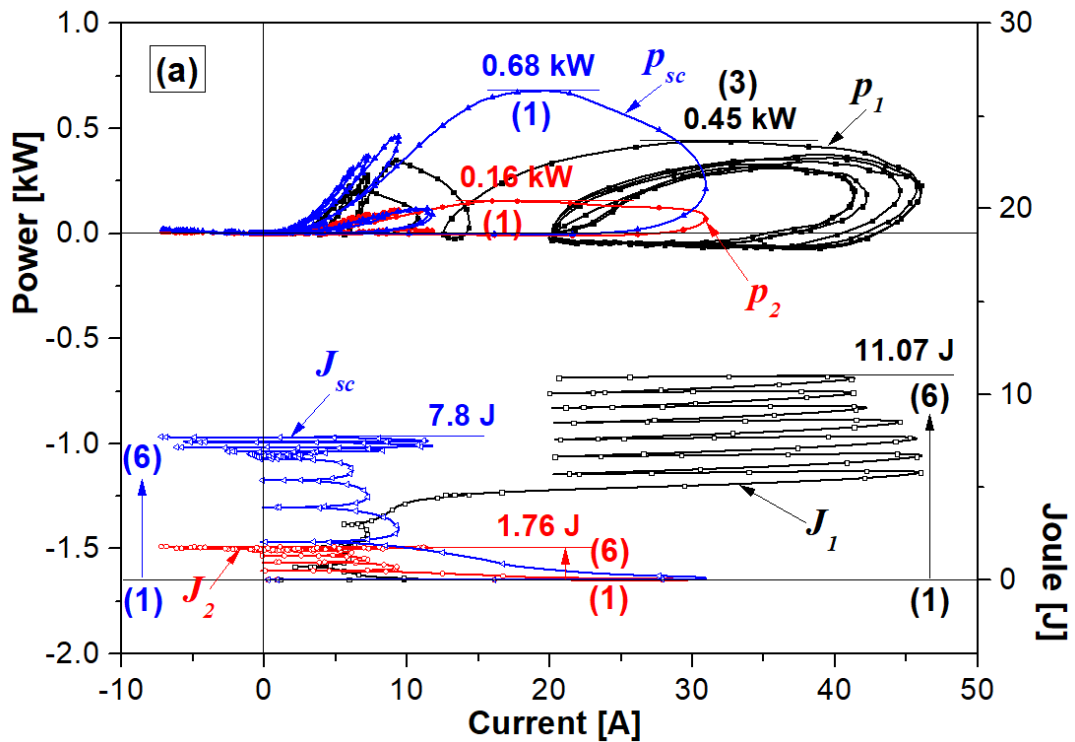


Figure 5. Instantaneous powers and magnetic flux in each winding of bridge type SFCL with a single HTSC element using flux-coupling according to the connection direction between N_1 and N_2 . (a) In the case of the subtractive polarity winding. (b) In the case of the additive polarity winding.

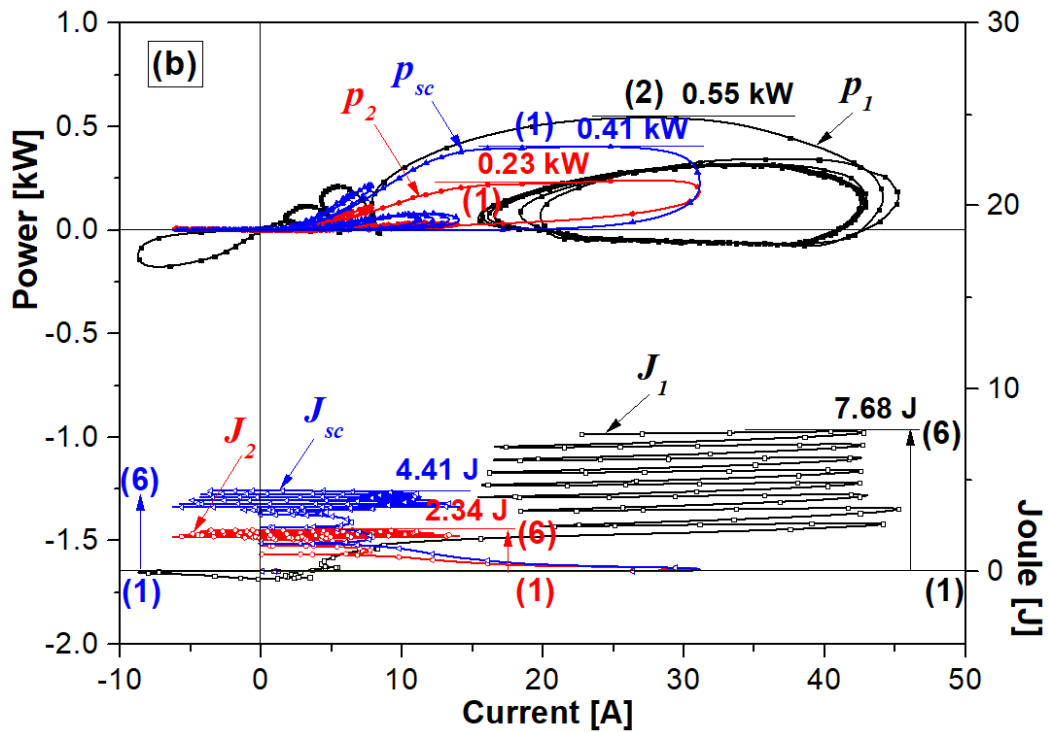
Figure 6 shows the power consumption and energy consumption of the HTSC element with respect to the current of a bridge type SFCL with a single HTSC element when the primary and secondary windings are connected as the subtractive polarity winding and the additive polarity winding during the fault period. In Figure 4, the fault sections (1), (2), (3), . . . , (6) displayed to subdivide the fault section are shown in the power consumption and energy consumption characteristics curve of each device. At this time, the power consumption characteristics of each device are displayed only on the maximum value of power consumption of each device because it is complicated to display the detailed failure section on each curve. When a fault occurs, the maximum power consumption of the HTSC element is 0.27 kW higher in the case of the subtractive polarity winding than that of the additive polarity winding, but the maximum power consumption of the primary and secondary windings is 0.1 and 0.07 kW less, respectively. During the fault cycle, the maximum energy consumption of the HTSC element is found to be 3.39 J higher in the case of the subtractive polarity winding than that of the additive polarity winding. It can be observed that the maximum energy consumed in the primary winding is as high as 3.39 J, while the maximum energy consumed in the secondary winding is as low as 0.58 J.

In brief, power consumption of each device was $P_{sc}^{sub} > P_{sc}^{add}$, $P_{1,max}^{sub} < P_{1,max}^{add}$, $P_{2,max}^{sub} < P_{2,max}^{add}$, and the energy consumption of each device was $J_{sc}^{sub} > J_{sc}^{add}$, $J_{1,max}^{sub} > J_{1,max}^{add}$, $J_{2,max}^{sub} < J_{2,max}^{add}$, respectively. The patterns of the power consumption and energy consumption of each device except the primary winding were the same. The maximum power consumption in the primary winding was higher in the case of the additive polarity winding than in the case of the subtractive polarity winding. The reason is that in the case of the additive polarity winding, the i_1 current flowing in the primary winding suddenly increased significantly at 1.5 cycles due to the voltage drop of v_1 . Conversely, the maximum energy consumption in the primary winding was higher in the case of the subtractive polarity winding than in the case of the additive polarity winding. The reason is that the range of power consumption of

the primary winding in the case of the subtractive polarity winding during 5.5 cycles of fault is more intensively concentrated than that in the case of the additive polarity winding.



(a)



(b)

Figure 6. Current vs. power consumption and energy consumption characteristics of each device according to the connection direction between N_1 and N_2 during the fault cycle. (a) In the case of the subtractive polarity winding. (b) In the case of the additive polarity winding.

4. Conclusions

In this paper, the fault current limiting characteristics, instantaneous power, and energy consumption of a bridge type SFCL with a single HTSC element were compared according to the wiring direction between the two coils during the fault period. Since the HTSC element operated under DC conditions, the fault current rapidly increased due to saturation of the iron core immediately after the fault occurred. However, it can be seen that the fault current is limited by the quenching of the HTSC element. It can be seen that the quench voltage of the HTSC element was much larger in the case of the subtractive polarity winding than that of the additive polarity winding. The instantaneous power dissipated in the single HTSC element was much larger in the case of the subtractive polarity winding than that of the additive polarity winding immediately after the fault. However, it could be confirmed that the instantaneous power consumed in the secondary winding was larger in the case of the additive polarity winding. In addition, the maximum energy consumed by the HTSC element during the fault period was higher in the case of the subtractive polarity winding than that of the additive polarity winding. At this time, the maximum energy consumed in the primary winding was higher in the case of the subtractive polarity winding, but the maximum energy consumed in the secondary winding was less. In conclusion, it can be confirmed that the modified bridge type SFCL with a single HTSC element had a fault current limiting operation function. Also, it can be confirmed that the power consumption and energy consumption of the HTSC element was lower in the case of the additive polarity winding than that of the subtractive polarity winding, and the fault current limiting characteristics were excellent. In the future, a basic study will be conducted on whether this modified bridge type SFCL model can be applied to a DC power distribution system.

Author Contributions: Writing-original draft, T.-H.H.; Designed the experiments and analyzed the experimental data; S.-C.K.; Writing-review and editing, S.-H.L. All authors have read and agreed to the published version of the manuscript.

Funding: This research was funded by Basic Science Research Program through the National Research Foundation of Korea (NRF) funded by the Ministry of education (2018R1D1A1B09083558) and funded by the Ministry of education (2018R1D1A1B07040471).

Conflicts of Interest: The authors declare no conflict of interest.

Nomenclature

SFCL	the superconducting fault current limiter
HTSC	the high temperature superconducting
N_1	the primary winding
N_2	the secondary winding
L_1	the inductance of the primary winding
L_2	the inductance of the secondary winding
I_{op-sub}	the fault current limiting operating current in the case of a subtractive winding
I_{op-add}	the fault current limiting operating current in the case of an additive winding
I_c	the critical current
E_{in}	the AC power supply voltage
X_{line}	the line reactance
R_{line}	the line resistance
R_{load}	the load resistance
i_b	the current of the bridge type SFCL
i_1	the current of the primary winding
i_2	the current of the secondary winding
I_{in}	the line current
V_1	the voltages induced by the primary winding
V_2	the voltages induced by the secondary winding

V_{SC}	the voltages induced by the HTSC element
R_{SC}	the resistances of HTSC element
ϕ_1	the magnetic flux of the primary winding
ϕ_2	the magnetic flux of the secondary winding
p_{SC}	the power of HTSC element
p_1	the power of the primary winding
p_2	the power of the secondary winding
J_{SC}	the joule energy of HTSC element
J_1	the joule energy of the primary winding
J_2	the joule energy of the secondary winding

References

- Hassenzahl, W.V.; Hazelton, D.W.; Johnson, B.K.; Komarek, P.; Noe, M.; Reis, C.T. Electric power applications of superconductivity. *Proc. IEEE* **2004**, *92*, 1655–1674. [\[CrossRef\]](#)
- Yuan, X.; Tekletsadik, K.; Kovalsky, L.; Bock, J.; Breuer, F.; Elschner, S. Proof-of-concept prototype test results of a superconducting fault current limiter for transmission-level applications. *IEEE Trans. Appl. Supercond.* **2015**, *15*, 1982–1985. [\[CrossRef\]](#)
- Lee, H.Y.; Asif, M.; Park, K.H.; Lee, B.W. Feasible application study of several types of superconducting fault current limiters in HVDC grids. *IEEE Trans. Appl. Supercond.* **2018**, *28*, 1–5. [\[CrossRef\]](#)
- Ko, S.C.; Lim, S.H. Analysis on magnetizing characteristics due to peak fault current limiting operation of a modified flux-lock-type SFCL with two magnetic paths. *IEEE Trans. Appl. Supercond.* **2016**, *26*, 1–5. [\[CrossRef\]](#)
- Lim, S.H.; Ko, S.C.; Han, T.H. Analysis on current limiting characteristics of a transformer type SFCL with two triggering current levels. *Phys. C Supercond. Appl.* **2013**, *484*, 253–257. [\[CrossRef\]](#)
- Abramovitz, A. Survey of solid state fault current limiters. *IEEE Trans. Power Electron.* **2011**, *27*, 2770–2782. [\[CrossRef\]](#)
- Boenig, H.; Paice, D. Fault current limiter using a superconducting coil. *IEEE Trans. Magn.* **1983**, *19*, 1051–1053. [\[CrossRef\]](#)
- Bock, J.; Hobl, A.; Schramm, J.; Krämer, S.; Jänke, C. Resistive superconducting fault current limiters are becoming a mature technology. *IEEE Trans. Appl. Supercond.* **2015**, *25*, 2880–2887. [\[CrossRef\]](#)
- You, H.; Jin, J. Characteristic analysis of a fully controlled bridge type superconducting fault current limiter. *IEEE Trans. Appl. Supercond.* **2016**, *26*, 1–6. [\[CrossRef\]](#)
- Hekmati, A. Proposed design for a tunable inductive shield-type SFCL. *IEEE Trans. Appl. Supercond.* **2014**, *24*, 1–7. [\[CrossRef\]](#)
- Li, B.; Jing, F.; Li, B.; Chen, X.; Jia, J. Study of the application of active saturated iron-core superconducting fault current limiters in the VSC-HVDC system. *IEEE Trans. Appl. Supercond.* **2018**, *28*, 1–6.
- Kumar, P.; Shaw, P. Comparison of superconducting fault current limiter topologies based on power electronic devices. In Proceedings of the 2016 7th India International Conference on Power Electronics, Patiala, India, 17–19 November 2016; pp. 1–5.
- Ghanbari, T.; Farjah, E.; Tashakor, N. Thyristor based bridge-type fault current limiter for fault current limiting capability enhancement. *IET Gener. Transm. Distrib.* **2016**, *10*, 2202–2215. [\[CrossRef\]](#)
- Jiang, L.; Jin, J.X.; Chen, X.Y. Fully controlled hybrid bridge type superconducting fault current limiter. *IEEE Trans. Appl. Supercond.* **2014**, *24*, 1–5.
- Baimel, D.; Tapuchi, S.; Baimel, N. New control strategies for IGBT based bridge type SFCL. In Proceedings of the 2018 IEEE 18th International Power Electronics and Motion Control Conference (PEMC), Budapest, Hungary, 26–30 August 2018; pp. 401–405.
- Radmanesh, H.; Fathi, H.; Gharehpetian, G.B. Series transformer based solid-state fault current limiter. *IEEE Trans. Smart Grid* **2015**, *6*, 1983–1991. [\[CrossRef\]](#)
- Arathi, T.O.; Reji, P. IGBT based bridge type fault current limiter. In Proceedings of the 2018 International CET Conference on Control, Communication, and Computing (IC4), Thiruvananthapuram, India, 5–7 July 2018; pp. 89–94.

18. He, J.; Li, B.; Li, Y. Analysis of the fault current limiting requirement and design of the bridge-type FCL in the multi-terminal DC grid. *IET Gener. Transm. Distrib.* **2017**, *11*, 968–976. [[CrossRef](#)]
19. Rashid, G.; Ali, M.H. A modified bridge-type fault current limiter for fault ride-through capacity enhancement of fixed speed wind generator. *IEEE Trans. Appl. Supercond.* **2014**, *29*, 527–528.
20. Abdolkarimzadeh, M.; Heris, M.N.; Abapour, M.; Sabahi, M. A bridge-type fault current limiter for energy management of AC/DC microgrids. *IEEE Trans. Appl. Supercond.* **2017**, *32*, 9043–9050. [[CrossRef](#)]
21. Imparato, S.; Morandi, A.; Martini, L.; Bocchi, M.; Grasso, G.; Fabbri, M.; Negrini, F.; Ribani, P.L. Experimental evaluation of AC losses of a DC restive SFCL prototype. *IEEE Trans. Appl. Supercond.* **2010**, *20*, 1199–1202. [[CrossRef](#)]
22. Morandi, A.; Brisigotti, S.; Grasso, G.; Marabotto, R. Conduction cooling and fast recovery in MgB₂-based DC resistive SFCL. *IEEE Trans. Appl. Supercond.* **2013**, *23*, 5604409. [[CrossRef](#)]
23. Wanmin, F.; Wu, B. A novel topology of bridge-type superconducting fault current limiter. In Proceedings of the 2009 Canadian Conference on Electrical and Computer Engineering, St. John's, NL, Canadian, 3–6 May 2009; Volume 21, pp. 2201–2204.
24. Hu, Y.; Xun, J. Analysis of a IGBTs-based bridge type superconducting fault current limiter. In Proceedings of the 2015 IEEE International Conference on Applied Superconductivity and Electromagnetic Devices (ASEMD), Shanghai, China, 20–23 November 2015; pp. 21–22.
25. Sadi, M.A.H.; Ali, M.H. A fuzzy logic controlled bridge type fault current limiter for transient stability augmentation of multi-machine power system. *IEEE Trans. Power Syst.* **2016**, *31*, 602–611. [[CrossRef](#)]
26. Lim, S.H.; Cho, Y.S.; Choi, H.S.; Han, B.S. Improvement of current limiting capability of HTSC elements in hybrid type SFCL. *IEEE Trans. Appl. Supercond.* **2007**, *17*, 1807–1810. [[CrossRef](#)]
27. Lim, S.H.; Kim, J.C. Quench and recovery characteristics of series-connected resistive type SFCLs with magnetically coupled shunt-reactors. *IEEE Trans. Appl. Supercond.* **2008**, *18*, 729–732.
28. Lim, S.H.; Choi, H.S. Quench characteristics of HTSC elements in series-connected flux-lock type SFCLs through magnetic flux-linkage. *Phys. C Supercond. Appl.* **2006**, *445–448*, 1073–1077. [[CrossRef](#)]



© 2020 by the authors. Licensee MDPI, Basel, Switzerland. This article is an open access article distributed under the terms and conditions of the Creative Commons Attribution (CC BY) license (<http://creativecommons.org/licenses/by/4.0/>).